Journal of Simulation and Analysis of Novel Technologies in Mechanical Engineering
16 (1) (2024) 0049~0057

Research article

Experimental study of turbulent wind flow over arc roofs: An ancient simple way to low energy buildings

Farhad Raeiszadeh, Mehdi Jahangiri*

Energy and Environment Research Center, Shahrekord Branch, Islamic Azad University, Shahrekord, Iran

*mehdi_jahangeri@yahoo.com

(Manuscript Received --- 14 Nov. 2023; Revised --- 14 June 2024; Accepted --- 30 June 2024)

Abstract

In hot, dry areas around the world, buildings are planned to shield against strong winds and to offer natural cooling during the summer. Many of these structures have curved or domed roofs, like arcs, vaults, or semi-circles. This paper presents an experimental study of air flow over arc roofs mounted over a flat surface with various diameters (80, 120, and 200 mm) at different flow velocities (5, 10, and 15 m/s). For this aim, models of half circle shape with the same length and different diameters have been made and installed in a subsonic wind tunnel. Using a vertical hot wire probe, measurements were conducted to analyze flow characteristics, which included mean flow velocity directions, root mean square values representing turbulent fluctuations, and the skin friction coefficient. These measurements helped in establishing the fluid pattern over the vault. Also, it was found that with increasing Reynolds number, fluid characteristics such as separation angle, recirculation length are increasing and location of maximum velocity remains almost constant. Results of experimental measurements are compared with flat roofs data and better thermal performance of arc roofs is observed.

Keywords: Reverse flow, Recirculation, Arc roof, Hot wire, Separation

1- Introduction

Wind has been utilized to improve indoor summer comforts in south and central part of Iran and Middle East region for more than several centuries [1]. In these areas, arc-shaped, domed, or vaulted roofs have conventionally been widely employed to shield buildings from intense sunlight and the resulting heat transfer. For passive cooling propose. The design of dwelling quarters as well as city fabrics in many desert communities in the Middle East have special arrangement with respect to wind. Yazd Province, located in the central region of Iran, includes some of the most ancient urban settlements, with history of more than 1000 years. Schematic of wind flow pattern and solar radiation with its shading is illustrated in Fig. 1 [2].

In recent years, significant research efforts have been directed towards low-energy buildings. These studies involve modeling and numerical simulations of passive cooling systems, revealing the pivotal role

of airflow in and around these structures in thermal analyses [3].

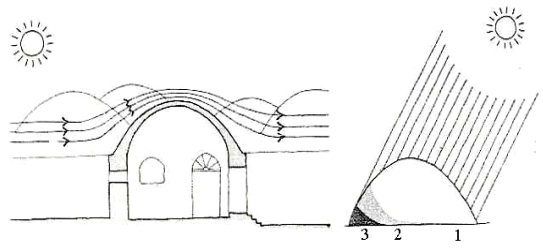

Fig. 1 A typical large house with schematic of sun shine and wind flow pattern

Yaghoubi and Velayati [4] carried out a computational study analyzing the wind flow behaviors around buildings featuring vaulted roofs of different shapes. Their analysis was based on assuming steady turbulent airflow, and they illustrated the flow patterns and pressure distributions around these structures, contrasting them with buildings having flat roofs. Their results validated that the notable pressure differentials identified in domed roofs notably augment passive ventilation and natural convection cooling, irrespective of the building's architectural design. Consequently, this circumstance leads to reduced indoor air temperatures compared to buildings with flat roofs, especially during hotter daytime conditions.

Abohela et al. [5] investigated the effect of different roof shapes by CFD simulation and they found that if arc roofs are chosen in the right direction of the wind, 56.1% of electricity consumption will be reduced.

Ozman et al. [6] conducted a study on turbulent flow patterns over models of low-rise buildings featuring gabled roofs with varying pitch angles. Through wind tunnel experiments and numerical analysis, they found that a roof pitch of 15º experiences more pronounced suction forces on the roofs compared to pitches of 30º and 45º. Notably, these angles are akin to the shape of an arc roof.

Shan et al. [7] investigated key characteristics of traditional Chinese architecture, which include curved slope profiles, elevated ridges, and layered roofs. They suggested that these aspects impact wind pressures and loads on roofs. Specifically, the curvature of a gabled roof can amplify the maximum area-averaged pressure and augment the resultant lift force.

From the above review dealing with domed or vaulted roofs, there is no experimental study for turbulent flow over an arc or vaulted roofs surrounded by flat surfaces. In continuation of previous studies, this paper aims to complement and expand upon existing research by offering additional experimental data, particularly focusing on the recirculation zone behind the roof. It will also explore the impact of the Reynolds number and roof diameter on the skin friction coefficient when air uniformly approaches from the flat area of surrounding roofs. The experiments involve the use of air as the test fluid, covering a velocity range that has been previously investigated by other researchers [4] and [8]. These experiments assume an incompressible fluid condition and adhere to the flow geometry depicted in Fig. 2.

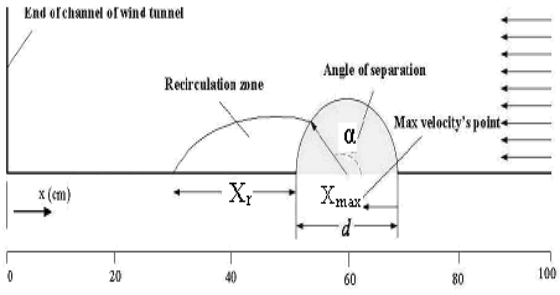

Fig. 2 Roof geometry used in the present study

2- Equipment and Methodology Used in Experiments

The experimental setup involves the utilization of an open-circuit blower-type low-speed wind tunnel which is shown in Fig. 3a. (Plint and Partner LTD model TE44) to replicate uniform airflow conditions. The test section has dimensions of 457mm × 457mm in cross-section and a length of 1200mm. Hot-wire anemometry was employed to conduct the experiments. To ensure accurate positioning of the hot-wire probe in both the streamwise, cross-streamwise, and vertical directions, a specialized traversing mechanism (specifically, model 57H00 from Dantec Co.) was installed. Fig. 4 depicts a schematic diagram of the experimental setup and the traversing mechanism. A dedicated structure was devised and secured to the ground to affix the traversing mechanism onto the wind tunnel, as depicted in Fig. 4. The measurement devices encompass a Constant Temperature Anemometer (CTA) that integrates a Wetson Bridge, linearizer, and signal conditioner. The output signal is transmitted via an A/D digital card to the connected computer, using the Keithley Metrabyte model DAS-1600 card capable of operating at a speed of 100 KHz. Data analysis was conducted through a specialized program named Streamline, provided by Dantec Co.

a)

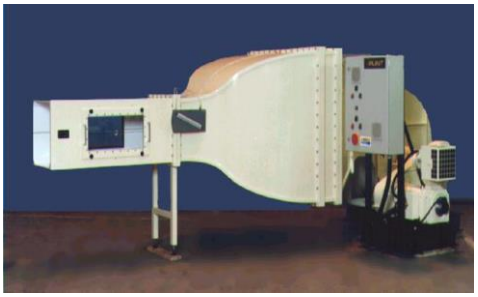

b)

Fig. 3 a) Wind tunnel set-up, b) Model with probe and traversing system

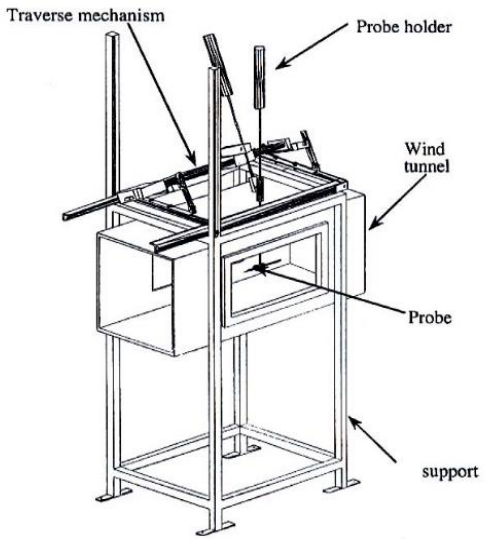

Fig. 4 Schematic of the experimental device used in the present work

The software is tailored to interact with the CTA, control the hot-wire probe, conduct analysis, and store the gathered data using the probe's specific calibration curve [9]. Fig. 3b depicts a model in test section with probe and traversing system. The models were made from polyetilen. The size of the models was 456mm length and various diameters of 80, 120 and 200mm. The experiments utilized hot-wire anemometry. To ensure precise positioning of the hot-wire probe in the streamwise, cross-streamwise, and vertical directions, a specialized traversing mechanism was installed. For probe movement over the vault, a 4cm wide open slot was introduced on the upper side of the wind tunnel. The positioning of the probe in the streamwise

and cross-stream directions could be adjusted in increments of 0.05 mm through computer control. For measuring mean velocity, the hot wire was oriented at a 90º angle to the flow direction within a plane parallel to the vault surface. During these measurements, the anemometer operated with a linearizer.

3- Methodology

The turbulent intensity and velocity field were assessed by displacing a hot-wire probe with the aid of an automated traversing system. The primary component of this mechanism was located above the wind tunnel, as shown in Fig. 4. The probe and its supporting structure were the only parts extending into the flow field. Furthermore, the stability of the mechanism was evaluated, ensuring the absence of any vibrations induced by the flow. Velocity vectors were determined by converting the measured voltage via calibrator curve for each experiment. Traversing mechanism is moved both horizontally and vertically at the place located at mid-position of the test section of wind tunnel such that two-dimensional measurements started from a point very close to each surface less than 1mm. Then the traverse system is moved 1mm upward and measurement is repeated. It was observed that for a specific height, velocity approached to a zero value, such point is considered as the location that velocity direction changes as illustrated in Fig. 5. The step for streamwise movement of traverse mechanism is taken 1 cm. Measurements were taken at streamwise locations N_x, with each measurement involving a set of N_y points. Table 1 displays the counts of N_x and N_y recorded for different circular diameters (in cm) and flow velocities (in m/s).

Tests were conducted to assess the consistency of measurements under two distinct configurations, with a diameter (d) of 120 mm and a velocity (V) of 10 m/s. Results showed that the variance in mean velocity was under 1%, while the fluctuation in velocity was less than 3%. The sensor used in these tests was unable to register negative flow velocities; hence, all the recorded data signify instantaneous velocity, average velocity, and their variations, all represented with a positive voltage polarity. These values were subsequently transformed into speed using the calibration curve depicted in Fig. 6, and their directional vectors were aligned as per the guidance provided in Fig. 5.

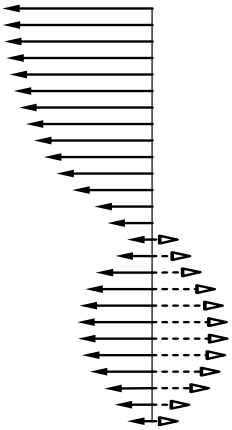

Fig. 5 Counter wise velocity vectors direction

Location of maximum air velocity X_{max} and variation of friction coefficient over the roof are parameters that accounts for analogy with convection heat transfer coefficient. The value of friction coefficient, C_f is determined by the following solution from experimental data [10].

$$\frac{C_f}{2} = \frac{0.168}{\left[ln\left(\frac{864\delta_2}{k_s}\right)\right]^2} \quad (1)$$

In this equation k_s is surface roughness which is determined from Nikoradze experiments and δ_2 is relative momentum displacement thickness computed from the following equation.

$$\delta_2 = \theta = \frac{1}{U_r^2}\int_0^{\infty} U_{mean}\,(U_r - U_{mean})\,dy \qquad (2)$$

U_r is the base velocity that located far from the model.

Table 1: Experimental measurements and number of selected points in each experiment

Experiment condition	Reynolds number	N_x	N_y
d=8, v=5	25173	8	60
d=8, v=10	50346	10	60
d=8, v=15	75519	11	60
d=12, v=5	37759	11	80
d=12, v=10	75519	15	80
d=12, v=15	113278	15	80
d=20, v=5	62932	18	100
d=20, v=10	125865	20	100
d=20, v=15	188797	20	100

4- Results and discussion

From hot-wire measurements, air flow pattern, flow separation and reattachment point over and around vault shape roofs surrounded by flat surfaces are determined. From these experiments, mean distribution of relative velocity, skin friction coefficient and reattachment regions for various Re_d are obtained.

For laminar cross flow over cylinder, separation angle is θ =80˚ and for turbulent flow θ=140˚ [11]. For the present measurement of turbulent flow over a semi-circular surface it was that for Re_d = 25173, θ =139.7˚. “Fig. 6” shows flow measurements on the leeward side of the semi-cylinder surface. Flow reversal and recirculation is illustrated. The same experimental results for Re_d =50346 is illustrated in “Fig. 7” Recirculation region is increased while separation angle is measured: θ =141.9˚.

Result of recirculation length (mm), separation point and x projection of the location of maximum velocity (mm) over the arc roofs are presented in Table 2 for various Reynolds numbers. These measurements show that the flow separation angle for a semi-cylinder attached over a flat surface has maximum difference of ±4 degrees compare with a full circular cylinder in a free stream flow.

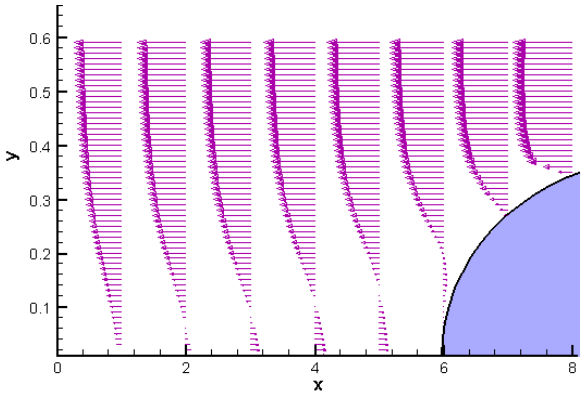

Fig. 6 Profiles of mean velocity, (d=8, v=5).

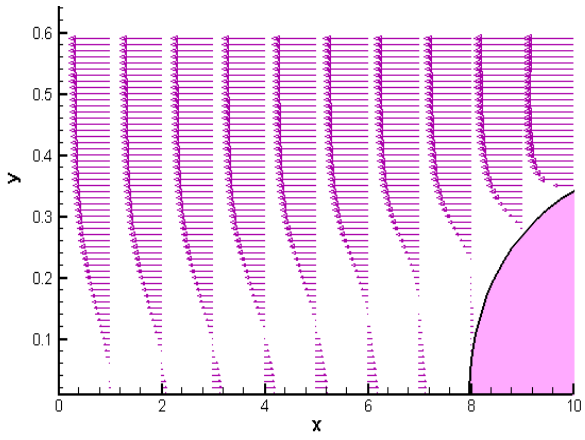

Fig. 7 Profiles of mean velocity, (d= 8, v=10).

Variation of C_f for an arc with d=120 mm and various Reynolds numbers is illustrated in Fig. 8. The pattern of C_f is the same for all Reynolds numbers but maximum value of C_f is increased by increasing air speed. Location of $C_{f\,max}$ and $C_{f\,min}$ is the same for all Re_d. Fig. 9 shows variation of C_f for various arc diameters and constant air speed of V=15m/s. The differences of C_f for d=80mm and d=120mm is not significant, only position of second maximum and second minimum shifted to the right direction. Similar changes are observed by increasing arc diameter to d=200mm

Table 2: Results of recirculation length, angle of separation, location of maximum air velocity over arc for various experiments (see Fig. 2)

Experiment condition	X_r	α	X_{max}
d=8, v=5	50	139.68	41
d=8, v=10	80	141.95	43
d=8, v=15	90	144.75	44
d=12, v=5	90	134.42	62
d=12, v=10	120	140.05	65
d=12, v=15	130	144.00	65
d=20, v=5	140	133.63	102
d=20, v=10	160	138.59	103
d=20, v=15	160	139.46	104

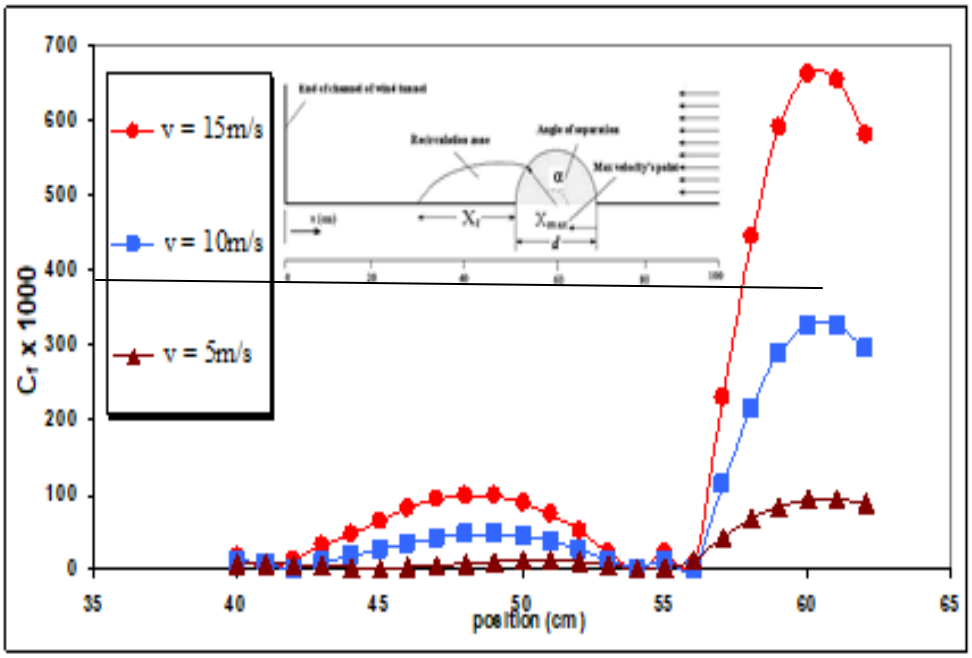

Fig. 8 Variation of C_f over arc roofs for various flow Reynolds numbers (d=120mm)

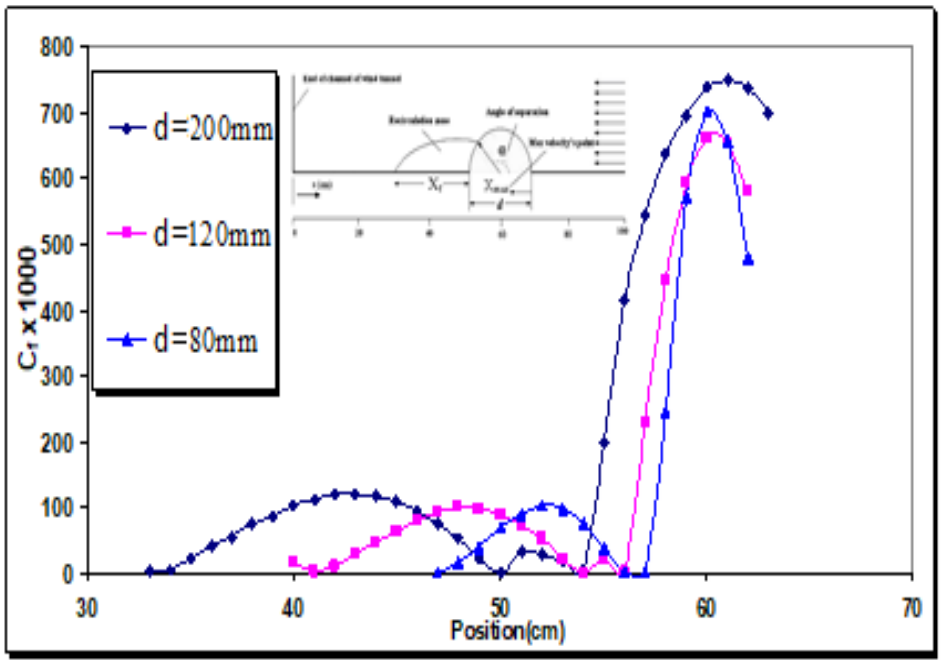

Fig. 9 Variation of C_f for various arc diameters (v=15 m/s)

Wind velocity on arc roofs is higher than flat roofs because for flat roof separation start at the leading edge while for vaulted roof, flow separation point takes place after top roof position [12]. This phenomenon can be clearly seen in Fig. 10.

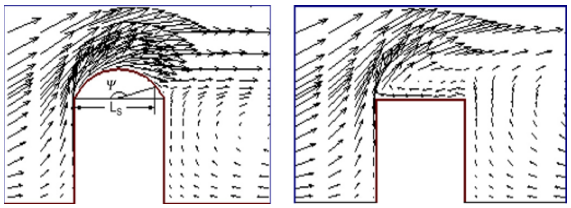

Fig. 10 Velocity vectors over arc and flat roof [12]

Higher wind velocity above the arc roof is one of the advantages of this type of roof in hot and dry areas. In areas where the wind blows, it reduces the intense heat entering the building due to radiation [13]. Comparison of experimental results for arc roofs and related flat roof data are illustrated in Table .3. As can be seen, at higher wind velocities, the difference between arc and flat roofs increases.

Table 3: Comparison of experimental results with flat roofs data of other researches

Authors	Present study		
	5 m/s	10 m/s	15 m/s
Hadavand [12]	4.5	-	-
Yu [17]	4.6 (num)	-	-
	4.8 (exp)		
Castelli [18]	-	-	12
Zhou [19]	3.9 (num)	-	-
	4.2 (exp)		
Ferreira [20]	-	8.5	-

5- Conclusion

A sequence of experiments was conducted to study the turbulent flow pattern over curved, circular arc roofs attached to a flat surface at different flow Reynolds numbers.

- For the same arc roof diameter, recirculation length increases with increasing Reynolds number as observed before [4].
- For the same arc roof diameter, angle of separation increases with increasing Reynolds number [11].
- For the same arc roof diameter, location of max velocity is about the crown of vault

and it does not vary by increasing Reynolds number.

- For the same Reynolds number, angle of separation decreases with increasing arc roof diameter.
- For the same roof diameter, the value of friction coefficient C_f increases with increasing Reynolds number [12-15].
- For the same Reynolds number, the value of C_f decreases with increasing roof diameter which confirms the results of previous research [12-16].

6- Suggestions for Future Work

For further work on the current article, the following suggestions are considered:

- Conducting additional experiments with different sizes of curved ceilings such as arches, vaults, or semicircles to examine the impact of various dimensions on the airflow patterns.
- Investigating the effect of air flow velocity on the thermal performance of curved ceilings and comparing it with flat ceilings.
- Performing numerical simulations using computational fluid dynamics software for a more precise analysis of airflow patterns over curved ceilings.
- Examining the influence of the shape and dimensions of curved ceilings on their thermal efficiency and heat transfer in different environmental conditions.
- Conducting further studies on the use of curved ceilings as sustainable and environmentally friendly building solutions in warm and dry regions.
- Utilizing some optimization tools such as neural network analysis.

References

[1] Shaeri, J., Habibi, A., Yaghoubi, M., & Chokhachian, A. (2019). The optimum window-to-wall ratio in office buildings for hot–humid, hot–dry, and cold climates in Iran. *Environments*, *6*(4), 45.

[2] Yaghoubi, M. A. (1991). Air flow patterns around domed roof buildings. *Renewable Energy*, *1*(3-4), 345-350.

[3] Bahadori, M. N. (1978). Passive cooling systems in Iranian architecture. *Scientific American*, *238*(2), 144-155.

[4] Yaghoubi, M., & Velayati, E. (2004). Analysis of wind flow around various domed-type roofs. *IMEC, Kuwait*, 209-217.

[5] Abohela, I., Hamza, N., & Dudek, S. (2013). Effect of roof shape, wind direction, building height and urban configuration on the energy yield and positioning of roof mounted wind turbines. *Renewable Energy*, *50*, 1106-1118.

[6] Ozmen, Y., Baydar, E. R. T. A. N., & Van Beeck, J. P. A. J. (2016). Wind flow over the low-rise building models with gabled roofs having different pitch angles. *Building and Environment*, *95*, 63-74.

[7] Shan, W., Yang, Q., Guo, K., & Tamura, Y. (2023). Effects of slope curvature, ridge height and layered roofs on wind pressures on traditional-Chinese-style gable-hip and gable roofs. *Journal of Building Engineering*, *70*, 106300.

[8] Yaghoubi, M., Kenary, A. and Mortazavi, M. Numerical Analysis of Wind Flow around Semi-circular Roof Buildings, Proceeding of 10th ISME, Khaje Nasir University, 2002.

[9] Yaghoubi, M., & Mahmoodi, S. (2004). Experimental study of turbulent separated and reattached flow over a finite blunt plate. *Experimental Thermal and Fluid Science*, *29*(1), 105-112.

[10] Kays, W. M., Crawford, M. E., & Weigand, B. (1980). *Convective heat and mass transfer* (Vol. 4). New York: McGraw-Hill.

[11] Shames, I. (2003). Mechanics of Fluids (4thedn) McGraw-Hill.

[12] Hadavand, M., Yaghoubi, M., & Emdad, H. (2008). Thermal analysis of vaulted roofs. *Energy and Buildings*, *40*(3), 265-275.

[13] Tang, R., Meir, I. A., & Wu, T. (2006). Thermal performance of non-air-conditioned buildings with vaulted roofs in comparison with flat roofs. *Building and Environment*, *41*(3), 268-276.

[14] Akbarpoor, A. M., Gilvaei, Z. M., Poshtiri, A. H., & Zhong, L. (2022). A hybrid domed roof and evaporative cooling system: thermal comfort and building energy evaluation. *Sustainable Cities and Society*, *80*, 103756.

[15] Pagnini, L., Delfino, F., Piccardo, G., & Repetto, M. P. (2023). Sustainability to wind

actions of a new roofing structure in a green university campus. *Building and Environment*, *245*, 110864.

[16] Dai, S. F., Liu, H. J., Chu, Y. J., Lam, H. F., & Peng, H. Y. (2022). Impact of corner modification on wind characteristics and wind energy potential over flat roofs of tall buildings. *Energy*, *241*, 122920.

[17] Yu, Z., Zhu, F., Cao, R., Chen, X., Zhao, L., & Zhao, S. (2019). Wind tunnel tests and CFD simulations for snow redistribution on 3D stepped flat roofs. *Wind and Structures*, *28*(1), 31-47.

[18] Castelli, M. R., Castelli, A., & Benini, E. (2012). Numerical Simulation of the Turbulent Flow over a three-Dimensional Flat Roof. *Engineeringand Technology*, *69*, 980-986.

[19] Zhou, X., Kang, L., Gu, M., Qiu, L., & Hu, J. (2016). Numerical simulation and wind tunnel test for redistribution of snow on a flat roof. *Journal of Wind Engineering and Industrial Aerodynamics*, *153*, 92-105.

[20] Ferreira, A. D., Thiis, T., Freire, N. A., & Ferreira, A. M. (2019). A wind tunnel and numerical study on the surface friction distribution on a flat roof with solar panels. *Environmental Fluid Mechanics*, *19*, 601-617.